

Research paper

Optimized mooring solutions for floating offshore wind turbines in harsh environments

Glib Ivanov^a, Yongyan Wu^{b,*}, Kai-Tung Ma^{a,**}^a Department of Engineering Science and Ocean Engineering, National Taiwan University, Taipei, Taiwan^b Aker Solutions Inc., 11700 Katy Freeway, Suite #1350, Houston, Texas 77079, USA

ARTICLE INFO

Keywords:

V-Share mooring
 Floating wind farm
 Optimal mooring design
 Shared anchor
 Shared mooring
 Polynomial regression analysis

ABSTRACT

The mooring system is a critical component of floating offshore wind turbines (FOWTs). Increased wind turbines in harsher environments necessitate larger mooring sizes and additional lines for redundancy. This study investigates the optimal mooring system for a three-column semi-submersible FOWT in Taiwan Strait, a region characterized by typhoon conditions. A novel mooring concept, V-Share Mooring, is introduced and compared against traditional clustered and spread mooring systems. The V-Share design connects two mooring lines from two columns of the semi-submersible to a single anchor. It utilizes all field-proven mooring components for reduced engineering risk and readiness. It is found that the V-Share mooring can stabilize the floater with smaller platform offset and yaw motions and may provide an opportunity to reduce the floater size. Using polynomial regression with response surface analysis of platform offset and mooring tension, optimal mooring design parameters, including pretension and total chain weight, are determined. A cost comparison provides an apples-to-apples assessment of total mooring procurement and installation expenses. Due to the anchor sharing, the V-Share system can be relatively cost-efficient, offering a reduced mooring footprint, minimized seabed disruption, and improved floater stability. The findings in the study may contribute to improving the economic viability of FOWTs.

1. Introduction

As the demand for decarbonization grows, offshore wind power is emerging as one of the most effective renewable energy solutions. However, most offshore wind resources are located in waters deeper than 60 m, where fixed-bottom foundations are not economically feasible. This makes floating offshore wind turbines (FOWTs) a crucial technology for unlocking vast offshore wind potential (Rehman et al., 2023) (Díaz and GuedesSoares, 2020) (Hong et al., 2024). Despite their advantages, FOWTs remain costly, limiting large-scale commercial deployment. A similar challenge once existed for fixed-bottom turbines, but their costs declined by over 50 % within a decade (Chang et al., 2022). One of the primary cost differences between fixed and floating wind turbines lies in the mooring system, which plays a critical role in both floater stability and overall system expenses.

Current mooring technology for FOWTs is largely adapted from offshore oil and gas practices (Ma et al., 2019), where each mooring line is typically secured to a dedicated anchor. For mooring line layout, they

are typically either clustered into three or four groups or nearly evenly distributed (Ma et al., 2019). However, offshore wind projects differ from oil and gas in that they are more economically and environmentally sensitive. As a result, conventional mooring solutions face technical and commercial challenges, requiring significant cost reductions to achieve commercial viability.

In addition to high costs, existing mooring systems present elevated environmental risks. Large mooring footprints may disrupt marine ecosystems and interfere with industries such as fisheries and maritime transport. Furthermore, mooring system reliability has proven to be lower than expected (Ma et al., 2019) (Ma et al., 2013). To enable cost-effective and sustainable FOWT deployment, a fundamental re-evaluation of mooring design for floating wind is necessary. This includes optimizing mooring layouts and patterns, exploring alternative materials, and developing innovative mooring components. The ultimate goal is to improve cost efficiency, reduce environmental impact, and enhance system reliability.

Academia and industry are actively exploring innovative mooring

* Corresponding author.

** Corresponding author.

E-mail addresses: yongyan.wu@akersolutions.com, wuyongyan@gmail.com (Y. Wu), kaitungma@ntu.edu.tw (K.-T. Ma).

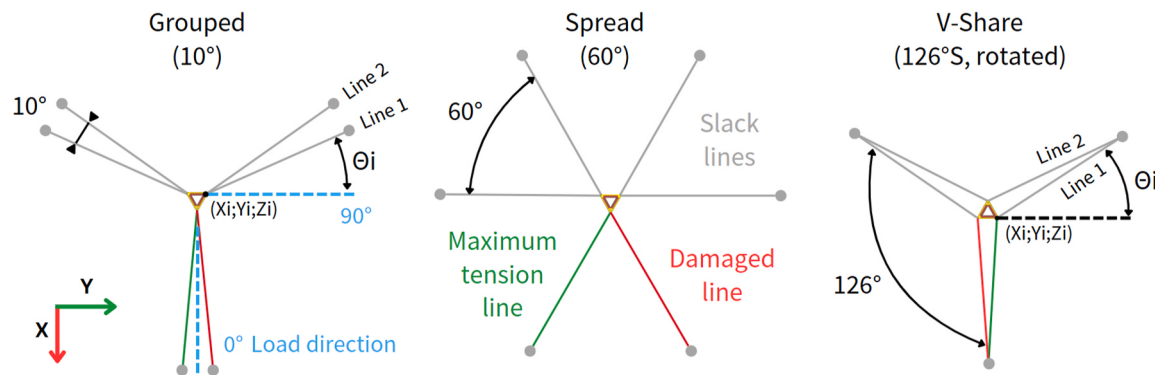


Fig. 1. Schematic representations of 3 mooring patterns, clustered, equal-spread, and V-share.

designs, advanced mooring material, and new mooring components to reduce mooring costs, increase installation and hook-up effectiveness, and ultimately reduce the environmental impact. Shared anchors and mooring lines between different floaters have been an emerging research topic as they are expected to reduce overall construction costs for large-scale floating wind farms (Xu et al., 2024). The basic concept of shared anchoring involves connecting multiple mooring lines from different floaters to a single anchor, reducing the total number of anchors while balancing horizontal forces across the system. Shared mooring lines can be configured as suspended mooring systems or as lines incorporating additional buoys and tethers connected to extra anchors. However, implementing a shared mooring system between different floaters introduces complexity to the dynamics of FOWTs, necessitating the development of advanced simulation tools to meet modelling requirements (Xu et al., 2024), on top of extra engineering concerns such as long term system reliability, sea surface interaction due to the near-surface shared mooring lines, damage tolerance (Ivanov and Poita, 2025), among many other practical engineering considerations that must be addressed for successful deployment in the ocean.

Designing an economical mooring system for relatively shallow water depths ranging from 60 m to 100 m is particularly challenging (Xu et al., 2021). This is because the mooring system must provide sufficient catenary geometric stiffness to minimize dynamic reactions, which often leads to an increased mooring footprint (horizontal mooring scope) and larger, heavier mooring chains. Unlike solitary oil production floaters, numerous floating turbines are being crammed into a small area, and the mooring footprint was shown to be the limiting condition on how close turbines can be spaced (Ma et al., 2025a) as opposed to the wake effect being the limitation of fixed-bottom turbines. Current academic and industry solutions for shallow water mooring focus on developing new mooring materials, such as HMPE or nylon ropes (Ma et al., 2019) (Fonseca et al., 2024), as well as innovative mooring components, such as load reduction devices (Aryawan et al., 2023). Nylon rope has been used in industry for a long time, mainly in lifting and temporary mooring. It offers greater flexibility than polyester rope for the same minimum breaking load, which can be advantageous for shallow water mooring systems. However, nylon's use in permanent mooring for floating structures currently remains limited, and challenges related to fatigue and fracture performance under long-term loading must be addressed. Similarly, while load reduction devices show promise, they currently lack substantial industry track records and face several practical engineering challenges, including concerns about their robustness in functioning as designed under both tension and fatigue. Therefore, for waters shallower than 100 m, catenary design remains a popular choice, particularly where installation simplicity, reliability, and proven performance are prioritized (Lozon et al., 2025).

This paper focuses on the design of mooring system layouts, recognizing that new mooring materials and components can be integrated into these systems once their technical readiness levels are sufficiently

mature for real ocean deployment. Specifically, we explore a new and simple mooring system called the V-Share mooring system (Wu et al., 2023). Unlike traditional shared mooring and anchor systems, where one anchor connects to mooring lines from multiple floaters (Xu et al., 2024), the V-Share mooring features two mooring lines from two columns of a semi-submersible floater, both connected to a single anchor. With over 50 years of industry experience in oil and gas, anchors have proven to be the most robust mooring component (Ma et al., 2019). Therefore, the use of a shared anchor within the same floater does not compromise system reliability. This paper examines how the V-Share mooring system influences mooring performance and platform motions.

This paper utilizes a new 15 MW semi-submersible FOWT, named TaidaFloat (Ivanov et al., 2023), in the Taiwan Strait at a water depth of 70 m to investigate various mooring system layouts, considering configurations including traditional clustered and spread moorings as well as the new V-Share mooring. The Taiwan Strait is known for its relatively strong winds and waves, particularly due to typhoon (tropical cyclone) activity, which presents significant challenges for the design and installation of offshore structures, as well as for mooring design (Ivanov et al., 2024a) (Ma et al., 2025a). TaidaFloat is specifically designed to withstand a 50-year return period typhoon. Designing mooring systems for typhoon-prone regions involves unique challenges, as cyclonic winds and waves can approach from any direction, requiring symmetrical and redundant mooring designs to ensure stability and robustness.

When investigating the V-Share mooring with a single floater, we focus on the relationship between mooring line spreading angles and floater motions. Essentially, we are investigating the mooring and floater motions by changing the mooring line spreading angles. Meng et al. (2021) studied the influence of large spreading angle variations, 45°, 60°, and 120°, on the movements of the floater, as opposed to the cost. They found that spread mooring (45° in their 4x1 case) resulted in minimum yaw motion, 4 times less than the yaw motion amplitude in other cases. Huang et al. (2024) used an off-center turbine floater and varied the spreading angle only slightly from 6° to 12° (angle definition in this paper). While they recorded tension reduction with this angle increase, they concluded that a smaller spreading angle is more appropriate, citing perceived ease of installation.

While the V-Share mooring system differs from traditional mooring primarily in heading angles, its key advantage lies in utilizing a shared anchor within the same floater. Therefore, a comprehensive, apples-to-apples comparison is essential to assess its overall benefits and potential drawbacks. This paper presents a preliminary cost analysis to evaluate the feasibility of the proposed mooring system.

Mooring system design is inherently complex, requiring careful trade-offs among various parameters, including mooring line pre-tension, length, and diameter. With advancements in computing technologies, big data analysis and machine learning techniques can now be leveraged to optimize design parameters (Shanock et al., 2010) (Yang

et al., 2023). Yu et al. (2024) proposed an intelligent optimization algorithms approach for the optimal design of asymmetrically moored floating structures, considering the mooring radius, azimuth, separate angle, number of lines, and segment lengths as design variables. In this study, we simplify the design process by focusing on an all-chain mooring system with a reasonable horizontal mooring scope to minimize wind turbine interactions. The key design variables are reduced to chain pre-tension and diameter. A 3-D response surface is generated using a brute-force evolutionary solver (Shanock et al., 2010) to determine the optimal mooring design parameters for cost comparison.

Rather than developing new simulation tools, we utilize the well-established commercial software OrcaFlex (Orcina, 2023) to model the fully coupled aero-hydrodynamic floater-mooring system. This approach ensures reliability by applying proven methods and tools while exploring the potential of an innovative mooring system. The findings from this study aim to provide valuable insights for both academia and industry, contributing to the advancement of floating wind engineering and technologies in harsh environments.

2. Mooring design and analysis: theory and methodology

2.1. Mooring systems of different patterns

The primary function of a mooring system is to provide restoring forces to keep a FOWT on the station under specific environmental conditions to allow for wind power generation. Therefore, this section starts with the mooring system restoring stiffness from a theoretical point of view to identify the theoretical background behind the proposed new mooring system, V-Share mooring. Eventually, we would rely on numerical simulation tools such as OrcaFlex (Orcina, 2023) to verify the prediction and expectation.

Mooring patterns can influence both mooring tension and floater motion. Without loss of generality, Fig. 1 illustrates three mooring configurations: (i) clustered mooring with three groups, each having a 10° separation angle (left), (ii) evenly distributed spread mooring (middle), and (iii) a configuration with the maximum possible spreading angle (right).

In engineering practice, a 10° separation angle is commonly used to allow sufficient installation tolerance, though smaller angles, such as 5°, may be feasible in certain cases. Real-world mooring design must account for installation tolerances, site-specific constraints such as steep slopes, and geometric hazards that may limit anchor placement. Therefore, a 10° separation serves as a practical starting point.

Evenly distributed mooring, the 60° spread as shown in the middle of Fig. 1, is also a popular choice in the traditional oil and gas industry. This type of mooring system is mainly driven by the design during one-line damage scenarios, especially when there are eight or nine mooring lines in total. However, unlike oil and gas platforms, floating offshore wind turbines (FOWTs) do not pose risks of human casualties or oil spills. As a result, the required safety factors for damaged conditions are lower for FOWTs (safety factor = 1.05) compared to oil and gas platforms (safety factor = 1.25). Consequently, the intact condition governs the mooring design for FOWTs, whereas the damaged condition is the primary consideration for oil and gas platforms. Without loss of generality, this study includes the 60° spread mooring configuration as another representative traditional mooring system for evaluation.

As the spread angle between two adjacent mooring lines increases, causing their anchors to converge at the same location, the system transitions into a V-Share mooring configuration, as illustrated on the right in Fig. 1. In the case study for the Taiwan Strait, the estimated spreading angle is 126°, with a 4° separation between the two lines sharing an anchor. However, the 126° configuration shown in Fig. 1 serves only as an example. The actual angle in a V-Share mooring may vary slightly depending on mooring line length, site-specific bathymetry, and real-world deployment conditions.

2.2. Mooring stiffness

The mooring system's primary function is to provide restoring forces and stiffness to the floater, ensuring station-keeping. Therefore, it is essential to analyze how the mooring configurations shown Fig. 1 impact the mooring system stiffness.

Consider a floater with n mooring lines; i denotes the mooring line number, with $1 \leq i \leq n$. Each mooring line, which may consist of chain, synthetic rope, or their combination, has a horizontal restoring stiffness k_{hi} and vertical stiffness k_{vi} on the floater. Note that the stiffness expressions provided here are simplified and represent an idealized, linear approximation. In reality, mooring stiffness is generally nonlinear and varies with line geometry, pretension, and environmental loading conditions.

Let us discuss how these stiffnesses, line heading angles, and connecting points impact the six degrees of freedom of floater motion.

The surge and sway mooring system stiffness are expressed as:

$$\text{Surge : } K_{11} = \sum_{i=1}^n k_{hi} \sin^2 \theta_i \quad (1)$$

$$\text{Sway : } K_{22} = \sum_{i=1}^n k_{hi} \cos^2 \theta_i \quad (2)$$

where θ_i is the horizontal angle between the mooring line i and the x-axis (azimuth angles).

Clearly, the mooring line heading θ_i affects the floater motion in both surge and sway. As seen from Eqs. (1) and (2) and Fig. 1, if Line 1 in the traditional mooring has the same azimuth angles as Line 2 in the V-Share mooring, the surge and sway stiffness provided by Line 1 will be exactly the same as Line 2 of the V-Share mooring.

If we denote each line point of connection to the hull, i.e. the fairlead location, as (x_i, y_i, z_i) , the mooring system yaw stiffness can be easily obtained through coordinate transformations in θ_i direction and can be expressed as:

$$\text{Yaw : } K_{66} = \sum_{i=1}^n k_{hi} (x_i \cos \theta_i - y_i \sin \theta_i)^2 \quad (3)$$

For example, in Fig. 1, for traditional mooring, the yaw stiffness in the x and y components relative to the floater center are in opposite directions, one in the clockwise direction and one in the anti-clockwise direction. For the V-Share mooring, the two components of the yaw stiffness will be in the same direction. Therefore, the V-Share mooring will increase mooring yaw stiffness and thus reduce the yaw motion.

The heave stiffness has two parts: the stiffness from the water plane area, and the stiffness from the mooring system.

$$\text{Heave : } K_{33} = \rho g A_w + \sum_{i=1}^n k_v \quad (4)$$

where ρ is water density, g the gravitational acceleration, A_w the floater water plane area. Typically, the water plane area stiffness is much larger than the stiffness from the mooring system. Eq. (4) also demonstrate that, for a given single line mooring configuration (the same k_i), the mooring line headings will not impact heave motion at all. The roll and pitch motions' stiffness can be expressed as the combination of the floater and the mooring system:

$$\text{Roll : } K_{44} = \rho g V \overline{GM_T} + \sum_{i=1}^n (k_{vi} y_i^2 - k_{hi} z_i^2 \cos^2 \theta_i) \quad (5)$$

$$\text{Pitch : } K_{55} = \rho g V \overline{GM_L} + \sum_{i=1}^n (k_{vi} x_i^2 - k_{hi} z_i^2 \sin^2 \theta_i) \quad (6)$$

where V is floater displacement volume, and $\overline{GM_T}$ and $\overline{GM_L}$ are the floater transverse and longitudinal metacentric height, respectively.

Table 1
Required safety factors for steel mooring lines in ABS Rules.

Loading Condition	Redundancy	Design Condition	Safety Factor
Design Load Cases	Redundant	Intact	1.67
		One-line damaged	1.05
		Transient, damaged	1.05
	Non-redundant	Intact	2.0
		Either	1.05
		Intact	1.05

Traditionally, the mooring system has a marginal impact on the heave, roll, and pitch motions of a floater, particularly in the oil and gas industry, where floaters typically have a large water plane area A_w and significant displacement V , as can be seen from Equations (4)–(6).

However, for floating wind turbines, the mooring system could impact the roll and pitch motions through different headings of the mooring lines. This is especially true for floaters with relatively small displacement and metacentric height, such as semi-submersibles, which typically have a smaller GM than spar floaters. The mooring system's influence on roll and pitch becomes more pronounced depending on the specific design of the floater. This will be further verified through numerical simulations.

2.3. Fully coupled numerical simulations

We utilize the well-established commercial software OrcaFlex (Orcina, 2023) to model the fully coupled aero-hydrodynamic floater-mooring system.

OrcaFlex is a general-purpose software widely used in both academia and industry for simulating the dynamic behavior of marine systems, including floating platforms and their mooring systems, and can model fully coupled aero-hydrodynamic interactions. It allows for the analysis of wind turbine systems, including the turbine, tower, and floating foundation, and their interaction with the ocean environment.

The floater was modelled as a vessel body in OrcaFlex with the equation of motion in the time domain

$$M(p, a) + C(p, v) + K(p) = F(p, v, t) \quad (7)$$

where: $M(p, a)$ is the system inertia load; $C(p, v)$ is the system damping load; $K(p)$ is the system stiffness load; $F(p, v, t)$ is the external load; p , v and a are the position, velocity and acceleration vectors, respectively; t is the simulation time.

The finite element method is used for mooring line modelling in OrcaFlex. The line is divided into a series of straight massless model segments with a node at each end, and each segment models only the axial and torsional properties of the line. It turns out that the axial force predominates in the mooring system. Each line segment is divided into

two subsegments, and the properties of each subsegment, such as the mass, weight, and buoyancy, are lumped to the neighboring node. For a mooring line idealized as a solid cylinder, the tension in the axial spring-damper at the center of each segment is the vector, whose magnitude is given by

$$T = EAe \quad (\text{axial stiffness}) - 2\nu(p_0 a_0) \quad (\text{external pressure effect}) \\ + k_{tt}\tau/l_0 \quad (\text{torque coupling}) + EAc \frac{dl}{dt} \frac{l}{l_0} \quad (\text{axial damping}) \quad (8)$$

where E is Young's modulus; A is cross-sectional area; e is total mean axial strain $= (l - l_0)/(\lambda l_0)$; l is instantaneous length of segment; λ is expansion factor of segment; l_0 is unstretched length of segment; ν is Poisson's ratio; k_{tt} is tension/torque coupling factor; τ is segment twist angle (in radians); c is line damping coefficient (in seconds).

For simplicity, we choose to use the standard IEA 15 MW wind turbine model, which has been built in OrcaFlex according to the original specification (IEA Wind TCP 37, 2020), as this study focuses on the mooring system and its impact on the floater motions, including tower bending moment. The aerodynamic loads on the wind blade are modelled via the Blade Element Momentum (BEM) model with blade pitch controlled by the external function provided by OrcaFlex (Orcina, 2023), but metocean data, including wind speed, wave, and current data, will be from data for the Taiwan Strait. The full wind field is modelled through TurbSim (Jonkman, 2016), which allows for variation of wind velocity in both space and time.

The wave loads and response were calculated in OrcaWave, a software module in OrcaFlex based on diffraction analysis via potential flow theory. Current drag is acting on the underwater part of the floater and air drag on the above-water part, drag coefficients established with the help of viscous flow CFD (Tong et al., 2023).

Table 2
Site environmental conditions for DLC 6.1

Wind/Wave/Current	50-Year return period
Wind speed at 150 m hub height (10-min average)	57 m/s
Wind spectrum	Full-field IEC Kaimal
Significant wave height (H_s)	12.7 m
Peak enhancement factor (γ)	2.08
Wave period (T_p)	11.8 s
Wave spectrum	JONSWAP
The current speed at the surface	1.59 m/s
Current profile	Power law method profile
Tides	3.13 m to -2.8 m
Water depth	70 m

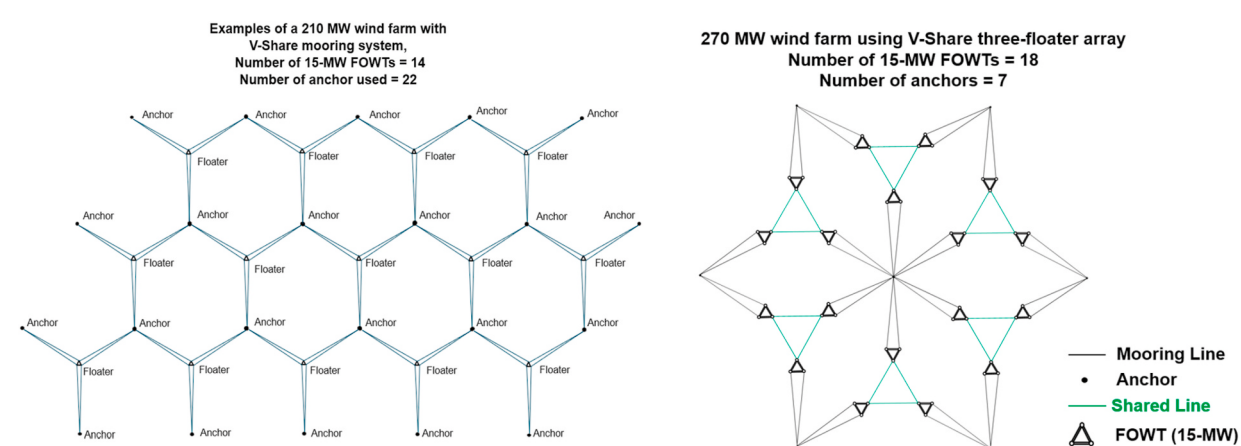


Fig. 2. Illustration of V-Share mooring in a wind farm.

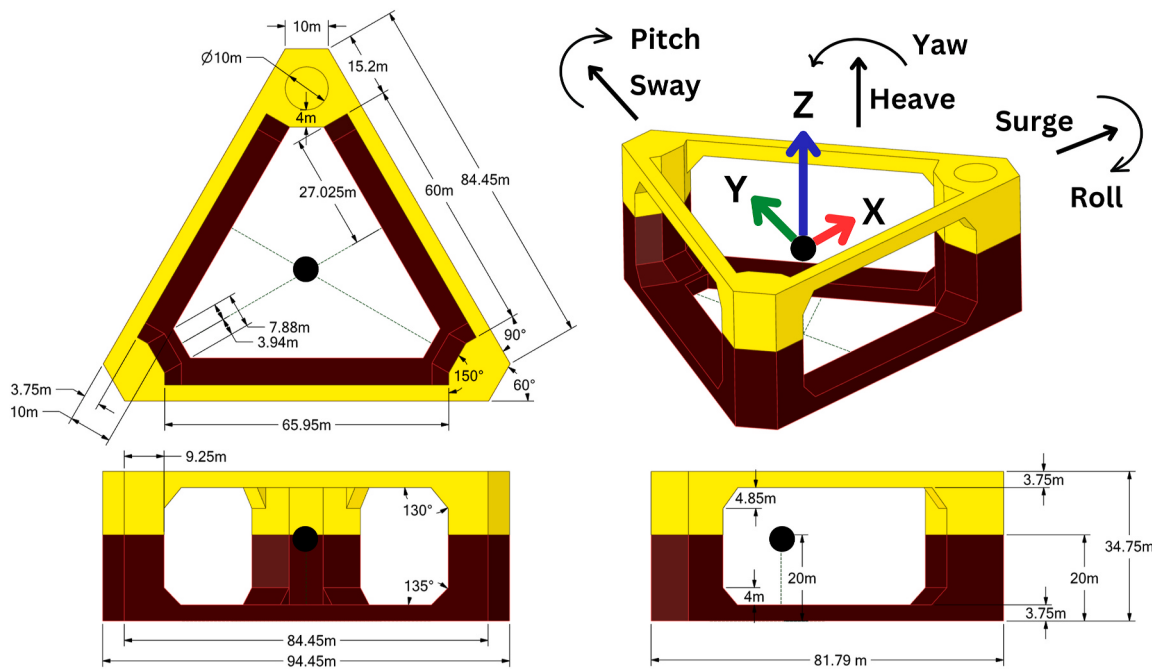


Fig. 3. TaidaFloat Semi-submersible hull composed of flat plates.

Table 3
Principal dimensions of the hull (TaidaFloat) and turbine (IEA 15 MW).

Parameter	Value
Hull Length (X-axis)	81.8 m
Hull Breadth (Y-axis)	94.2 m
Hull Height	34.75 m
Draught	20 m
Total displacement	20,300 t
Hull weight	4142 t
Rotor diameter	240 m
Turbine hub height	150 m
Blade mass	65.25 t
Tower mass	1263 t
RNA mass	991 t

2.4. Mooring parameters optimization methodology

The mooring system is defined by several key design parameters, including mooring pretension, line length, and component size. Changing the mooring configuration affects mooring performance, even when mooring line pretension and individual line profiles remain the same. A direct cost comparison between different mooring configurations that give different mooring performance would not be an “apples-to-apples” comparison. To enable a direct apple-to-apple cost comparison, it is essential to determine the optimal mooring parameters for each configuration.

In mooring design, two of the most critical performance indicators are maximum mooring tension and maximum platform offset. This study considers an all-chain mooring system, with the anchor-to-floater length pre-determined to prevent interaction with the floater. As a result, the two primary optimization parameters for each mooring pattern are mooring pretension and chain size. To achieve this optimization, we employ polynomial regression with response surface analysis (Shanock et al., 2010).

Polynomial regression with response surface analysis is an advanced statistical approach widely used in multisource feedback research (Shanock et al., 2010). This method allows for a detailed examination of how combinations of two predictor variables influence an outcome

variable, particularly when the interaction or discrepancy between predictors is of key interest.

The basic idea of polynomial regression is to model tension and offset as continuous functions of mooring pretension and chain size, as represented by the following polynomial equation:

$$Z = b_0 + b_1 X + b_2 Y + b_3 X^2 + b_4 XY + b_5 Y^2 \quad (9)$$

where Z represents either offsets or tension, X is mooring pretension, Y is the chain diameter, and b_0 , b_1 , b_2 , b_3 , b_4 , and b_5 are response surface coefficients.

To determine the response surface coefficients, more than five simulations are required. We used a brute-force evolutionary solver, which combines an exhaustive brute-force search with evolutionary algorithms to efficiently explore and optimize complex solution spaces. This solver was used to fit the data to Equation (9) (Shanock et al., 2010) and generate response surfaces for offset and tension. Based on these response surfaces, the optimal mooring pretension and chain size were determined, ensuring an objective and consistent comparison between different mooring configurations.

2.5. Design criteria and cost analysis methodology

The mooring system design in this study follows applicable regulatory guidelines, with the ABS mooring design code (ABS, 2020) serving as the primary standard, as shown in Table 1. The focus is on 3×2 mooring patterns, which incorporate redundancy to enhance reliability. Safety factors of 1.67 (intact) and 1.05 (damaged) are applied in accordance with ABS regulations. Given the historical challenges of mooring failures in offshore operations (Ma et al., 2021), redundant systems are designed to withstand one-line damaged scenarios (e.g., typhoons or collisions) while maintaining platform offset within safe limits to prevent damage to dynamic power cables.

The cost estimation methodology is structured as follows:

- Chain cost is calculated using Eq. (9), where material costs are a major contributor to total mooring expenses in 3×2 configurations.

$$\text{Cost}_{\text{chain}} = \text{weight} \times \text{unit price} \quad (10)$$

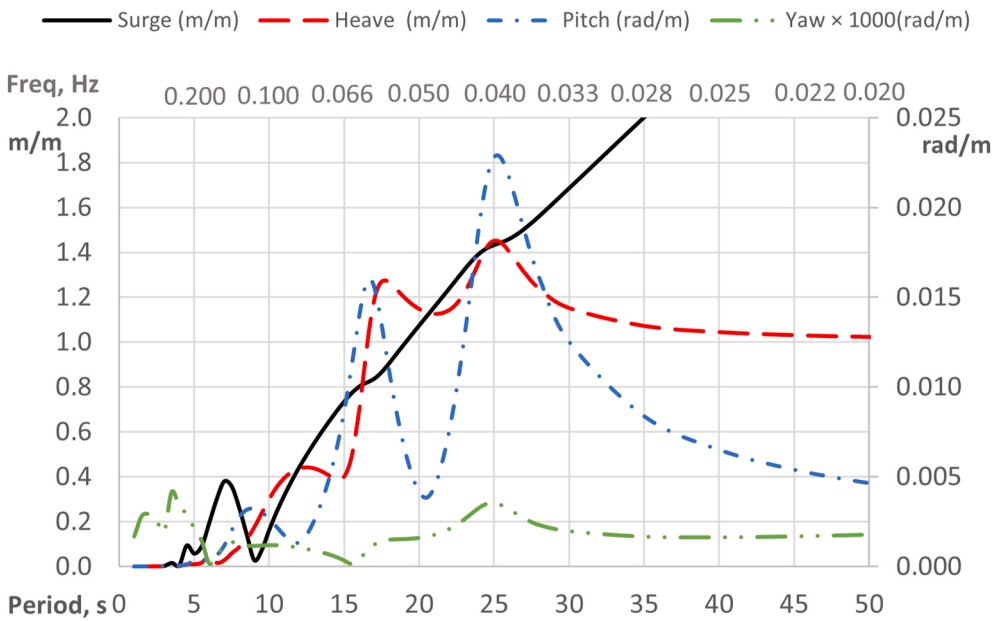


Fig. 4. Surge, heave, pitch, and yaw RAOs of TaidaFloat.

$$\text{weight} = \text{line length} \times \text{unit weight} \times \text{number of lines} \quad (11)$$

- Installation cost is based on project time data from Japanese floating wind developments compiled by T. Hasumi (Hasumi et al., 2023). The vessel charter rate for a large Anchor Handling Vessel is estimated and assumed at \$0.25M USD/day, and mooring chain costs are assumed at \$1500 USD/ton based on industry benchmarks.

While cost estimates can vary with market conditions, they serve as a useful baseline for evaluating the advantages and trade-offs of different mooring designs. To ensure a clear and unbiased comparison, the final cost analysis is presented in relative terms, using the total cost of the traditional mooring system as the 100 % reference point, with other configurations expressed as deviations from this baseline.

3. V-Share mooring system

The V-Share mooring system was first introduced to the industry in (Wu et al., 2023), featuring anchor sharing within the same floater. Its primary objectives are to reduce the number of anchors, along with associated installation costs and seabed footprint, while also contributing to improved platform motion performance.

For any novel technology, numerical simulation results alone hold limited value if significant engineering challenges hinder real-world deployment. The proposed V-Share mooring system is designed with practical implementation in mind, aiming for feasibility in offshore deployment beyond theoretical modeling.

This paper only studies stand-alone floater with the V-Share mooring and compares it to the traditional mooring. However, as an integral part of the broader engineering system, this section provides a comprehensive overview of the V-Share mooring from a practical engineering perspective, including mooring design and performance, installation and hookup, and impacts on the seabed and other maritime industries.

3.1. V-Share mooring system for a stand-alone floater

The V-Share mooring features two lines connecting two corners (columns) of a floater to one anchor. Fig. 1, right, shows a triangle-shaped floater with three columns moored by a six-line V-Share system to three anchors. For comparison, a traditional mooring system is

shown in Fig. 1, left, with a dedicated anchor for each mooring line. Compared with traditional mooring, which has a dedicated anchor for each mooring line, the V-Share mooring system has the following advantages:

- (1) Improved platform motion. The V-Share mooring system provides similar restoring forces to traditional mooring in surge and sway while offering higher yaw stiffness. It also reduces maximum heel angles by minimizing mooring-induced heeling moments in critical directions. This improved platform motion benefits FOWT development in several ways. For floater design, reduced heeling and yaw motions allow for smaller floaters with lower freeboards, enabling a lighter hull and a more compact mooring system, particularly in cases where the ultimate limit state (ULS) governs design. Additionally, lower yaw motion decreases load on the wind turbine tower, improving its structural integrity and longevity. Furthermore, if the V-Share mooring system also reduces heel angles during turbine operation, it may enhance wind turbine efficiency, which warrants further investigation in future studies.
- (2) The V-Share mooring system reduces the number of anchors, lowering environmental impact on benthic habitats and cutting costs associated with anchor materials, transport, installation, and geotechnical site investigations. Shared (multiline) anchors, which secure multiple mooring lines to a single anchor, allow for a significant reduction in the total number of anchors, further driving cost savings. Industry practice typically requires a detailed geotechnical survey at each anchor site to assess soil conditions, but with shared anchors, these survey costs are substantially reduced. Additionally, fewer anchors minimize seabed disturbances, decrease environmental impact on benthic habitats, and potentially shorten the duration and intensity of construction noise, reducing its impact on marine mammals.
- (3) Reduced mooring seabed footprint. The V-Share mooring reduces the seabed footprint, thus reducing the marine operating and maintenance (O&M) costs and decreasing the risk of submarine collision and entanglement of derelict fishing gear during O&M. Regular inspection and maintenance are recommended for the floating offshore wind mooring systems. Inspection vessels will need to move from one location to another, and Remotely Operated (underwater) Vehicles (ROVs) will conduct inspections

Table 4
Floater drag coefficients as input for Orcaflex.

	Current Drag		Wind Drag					
	Direction	Surge	Sway	Heave	Roll	Pitch	Yaw	Direction
Areas (m^2) and area moments (m^3) (A_i)	/	1225.9	872	2557	1.74E+04	2.45E+04	1.36E+05	/
Drag coefficients (C_d)	0	1.3	0.01	-0.37	0	-0.72	0	0
	30	0.94	0.19	-0.13	0.09	-0.46	0.02	30
	60	0.46	1.13	-0.5	0.51	-0.43	0.12	60
	90	-0.31	1.5	-0.2	0.68	0.03	0.16	90
	120	-0.62	1.5	-0.47	0.68	0.03	0.16	120
	150	-0.6	1.01	-0.14	0.46	0.18	0.11	150
	180	-0.87	0.02	-0.27	0.01	0.23	0	180
							-1.4	
						0.04	0.38	-0.03
							-0.95	0

along the mooring lines. Reducing the mooring system's footprint will reduce the vessel and ROV moving distance and relevant cost and maintenance schedule. Moreover, reducing the mooring system's footprint is likely to reduce the potential for secondary entanglement of whales.

The V-Share mooring system also provides an opportunity to reduce installation costs and improve hook-up efficiency through some innovative hook-up procedures. One way is to hook up two lines simultaneously to the same column of the platform. Only two hook-ups are required to achieve storm safety during the installation (Wu et al., 2023).

It is worth noting that connecting multiple mooring lines from a single anchor to different points on a vessel has been used in ship-shaped vessels moored to terminals. A similar concept has been applied to spars, where a bridle-like mooring configuration helps reduce yaw motion, as spars, being slender cylindrical structures, are naturally unstable in yaw. However, semi-submersibles differ significantly from spars in motion characteristics, construction, and installation. Therefore, the V-Share mooring is a new mooring system for semi-submersible floaters in harvesting wind energy. Furthermore, the installation advantages of the V-Share mooring system, as discussed earlier, further enhance its potential for widespread adoption in floating wind applications.

3.2. V-Share mooring system for floating wind farms

The advantages of the V-Share mooring for large-scale floating wind farms are more obvious compared to the stand-alone floater. As an example, the left of Fig. 2 shows a 210 MW wind farm with 14 15-MW floating wind turbines. The traditional mooring system will require 84 anchors. With the V-Share mooring by sharing anchors from different floaters in a honey-cone shape, the number of anchors will be reduced to 22 anchors, a reduction of 74 %, significantly reducing the anchor installation and maintenance costs and seabed interruption.

It is also possible to group multiple FOWTs and share mooring lines within the cluster. The right of Fig. 2 illustrates an example where three floaters are interconnected with shared suspended mooring lines between adjacent units. These suspended mooring lines will experience significant dynamic responses, and thus, load reduction devices might be needed to mitigate the excessive dynamic response. This mooring configuration introduces significant complexity in both numerical simulations and engineering practices, requiring further investigation to assess its feasibility, advantages, and potential challenges.

While multiple-turbine simulations have recently become feasible, they remain computationally demanding and complex to implement (Lozon et al., 2023). Moreover, not all mooring patterns examined in this study are compatible with anchor-sharing strategies. Therefore, only single-floater simulations are conducted in this work.

4. Floater and mooring model

4.1. Environmental conditions

The Taiwan Strait is characterized by strong winds, powerful currents, and frequent typhoons, making it a challenging environment for offshore structures. A generic metocean condition in the Taiwan Strait was applied in the numerical simulations. The water depth is 70 m flat. The mooring systems are checked against various design conditions, and the governing case is the extreme parked Load Case 6.1 as defined by ABS (ABS, 2020). The major site environmental conditions for the governing case are tabulated in Table 2. While DLC 1.6 is often considered critical in many regions, for this high wind-speed typhoon environment, DLC 6.1 was found to produce the governing loads in a previous study (Ivanov et al., 2024b), and is therefore adopted in this analysis.

The wind turbulence is simulated by the IEC Kaimal model within a

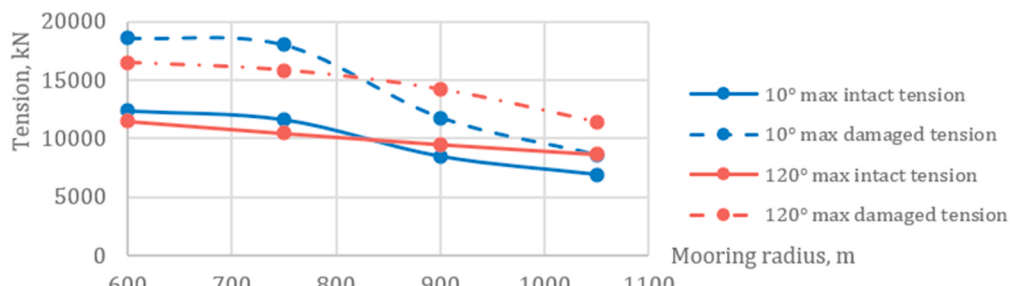


Fig. 5. Mooring tension change with mooring radius.

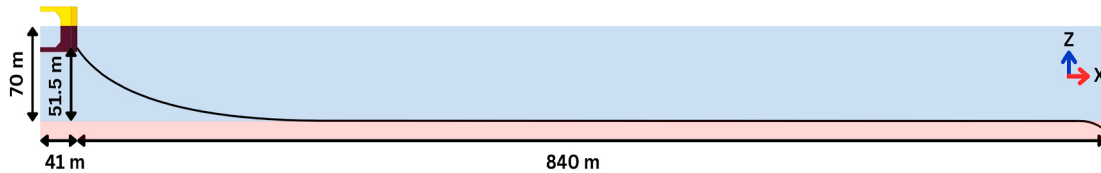


Fig. 6. Single mooring line profile.

Table 5
Single mooring line properties.

Parameter	Value
Mooring pattern	3 × 2 (Two lines on each column)
Chain grade	R4S Studless
Chain diameter (end of life)	160 mm
Chain MBL (end of life)	24281 kN
Chain corrosion allowance	4 mm/year
Anchor Radius	840 m
Design service life	25 years
Fairlead location	3.75 m above the keel

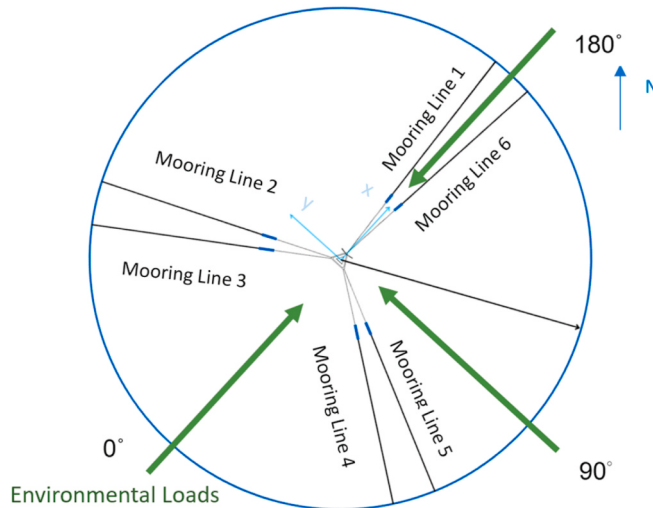


Fig. 7. Environmental heading and coordinate system.

full-field turbulence simulator, TurbSim, which is used to generate wind fields for wind turbine simulations (Jonkman, 2016). While DLC 6.1 typically includes misaligned wind and wave directions, this study adopts a simplified approach with colinear wind, wave, and current directions, meaning that the wind, wave, and current are aligned in the same direction for each single heading case.

4.2. TaidaFloat Semi-submersible

TaidaFloat is a three-hexahedral-column semi-submersible FOWT platform, optimized for efficient fabrication using flat plates, as shown in Fig. 3. It is designed to support large wind turbines, including 15 MW models, and withstand harsh marine conditions, such as typhoon-prone regions like the Taiwan Strait. The principal dimensions of the floater are as shown in Fig. 3 and also tabulated in Table 3, together with the wind turbine IEA 15 MW wind turbine principal dimensions. The tower is modelled based on the IEA 15 MW reference specifications and implemented in OrcaFlex (Orcina, 2023) using the Finite Element Method with 20 equally spaced beam elements. The tower base is rigidly connected to the floater, and wind loads are represented using drag coefficients applied according to the tower diameter.

The floater motion RAO (response amplitude operator) in heave and pitch are as shown in Fig. 4. The RAO damping is based on the 1:100 scale model tank test with individual regular waves (Lee et al., 2024), and the eigen periods are much higher than the environmental waves' peak period T_p 11.8 s. The double-peak phenomenon is due to the floater's columns being 2 different sizes. Table 4 shows the drag areas and coefficients for both current and wind. The drag loads are given by (Orcina, 2023):

$$F_i = \frac{1}{2} C_i \rho |\nu|^2 A_i \quad (12)$$

where F_i is the drag force or moment in six degrees of freedom, C_i is the drag coefficient, ρ is the water density or air density, ν is the relative velocity of the sea or air past the vessel, and A_i the areas or area moments in the six degrees of freedom.

4.3. The basic case mooring configuration

The moorings are attached to the TaidaFloat semisubmersible at 3.75 m above the keel. In this study, all chain mooring system is selected due to installation convenience. Although synthetic ropes or sheathed wire ropes are technically feasible at this water depth, they introduce additional challenges such as weak points at connectors, higher installation complexity, and increased project costs. Therefore, they are not preferred for the scope of this study.

Mooring radius is a key design factor. A larger radius reduces mooring tension but occupies more wind farm space, while a smaller radius increases turbine interaction risks due to wake effects. A previous study in the Taiwan Strait on a smaller semisubmersible (Lai et al., 2024)

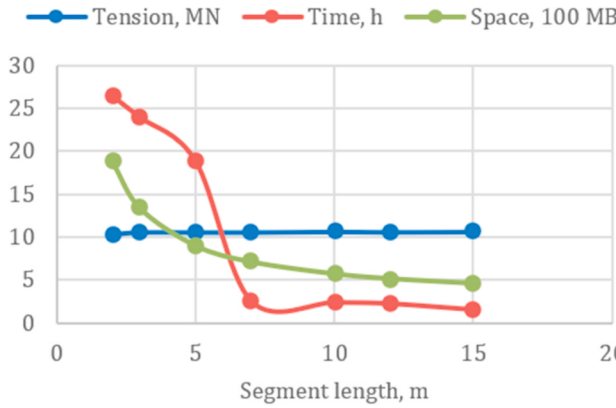


Fig. 8. Mesh (left) and seed (right) sensitivity of the mooring line modelled in OrcaFlex.

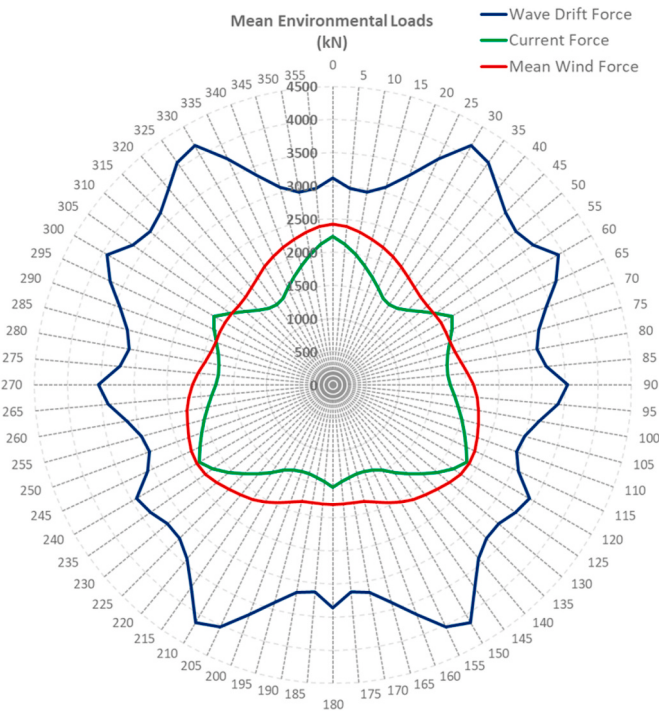


Fig. 9. Environmental loads on the floating system.

found that an 840 m radius provided a good balance between space utilization and tension reduction for 10° and 120° mooring headings, as shown in Fig. 5. In this study, an anchor radius of 840 m, approximately 12 times the water depth, is selected.

The mooring line profile are shown in Fig. 6 and Table 5. The base case mooring configuration for comparison consists of a 160 mm stainless chain. This setup serves as a reference to evaluating the impact of critical wave directions on mooring performance.

4.4. Coupled wind turbine, floater, and mooring model

Three key spreading angles, 10° clustered, 60° spread, and 126° V-Share mooring, are analyzed for their impact on platform offset and line tension, as shown in Fig. 1. The environmental heading and coordinate system are illustrated in Fig. 7.

For all simulations, at least 10 seeds were evaluated for each parameter set, with a simulation duration of 3 h (10,800 s). A mesh sensitivity study was conducted on the chain element length, along with a seed sensitivity analysis using different wave seeds. Fig. 8 presents the

results, showing that good convergence was achieved at 10 seeds and a 10 m segment length, which was adopted for numerical simulations.

The tension, offset, and tower bending moment are reported as Most Probable Maximum (MPM) values, in accordance with ABS code requirements (ABS, 2020).

The offset limit is set at 20 m, equivalent to 28 % of the water depth, as exceeding this threshold could damage the dynamic power export cable.

5. Results and discussions

5.1. Mooring performance and floater motions

This section examines and compares the mooring performance of three different configurations: 10° Clustered, 60° Spread, and 126° V-Share mooring. Fig. 9 illustrates the mean environmental loads from waves, currents, and wind across all directions, from 0° to 360° in 5° increments. Since environmental loads are independent of mooring configurations and exhibit symmetry along the 0°–180° axis, numerical simulations were conducted only for 0°–180°, with results for 180°–360° inferred by symmetry. As shown in Fig. 9, wave drift forces significantly exceed mean wind and current forces, indicating that this load case is predominantly wave-force driven.

The primary function of the mooring system is to limit platform offset, the displacement from the initial position. As shown in Fig. 10, offset results demonstrate the system's effectiveness in achieving this objective. Offset is directly linked to pre-tension, with all mooring lines pre-tensioned to 8 % of MBL in simulations. Initially, offset is constrained by the catenary shape of the mooring chain, as the floater must overcome the weight of the suspended segment before further displacement occurs. Once the chain becomes taut, additional offset is restricted, and tension rises rapidly.

Offset results, presented in Fig. 10, show significant variation depending on wave direction. The 10° clustered case exhibits the highest peak offset, while the 126° V-Share mooring case records the lowest offset at that wave heading, and vice versa. This suggests that mooring configurations should be optimized based on prevailing wind farm conditions. The maximum offsets for the 10° Clustered, 60° Spread, and 126° (V-Share) cases are 16.9 m, 14.0 m, and 15.7 m, respectively. Among these, the 60° spread mooring results in the smallest maximum offset, whereas the 10° clustered case produces the highest.

Fig. 10 also presents the maximum mooring tensions under different mooring patterns. The maximum tensions are 23476 kN, 21006 kN, and 27796 kN under the 10° clustered, 60° spread, and 126° V-Share mooring configurations, respectively. The 60° configuration exhibited the lowest maximum tension.

Yaw motion is a critical factor in offshore wind platform design, significantly impacting wind turbine reliability and tower structural

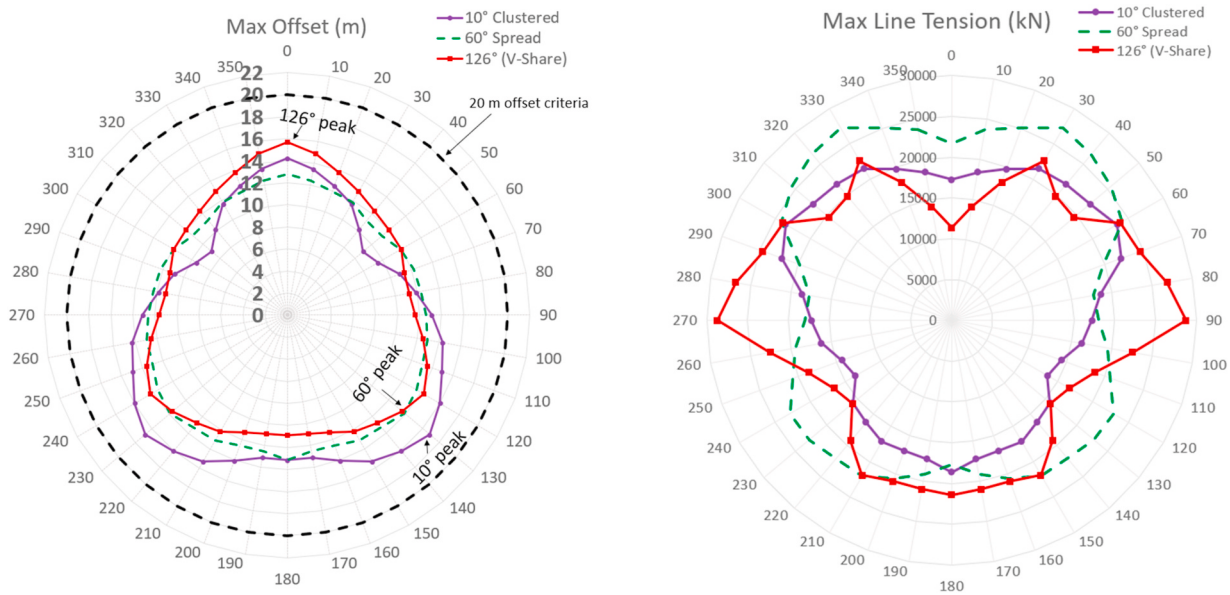


Fig. 10. Maximum platform offsets and mooring tension under three mooring patterns.

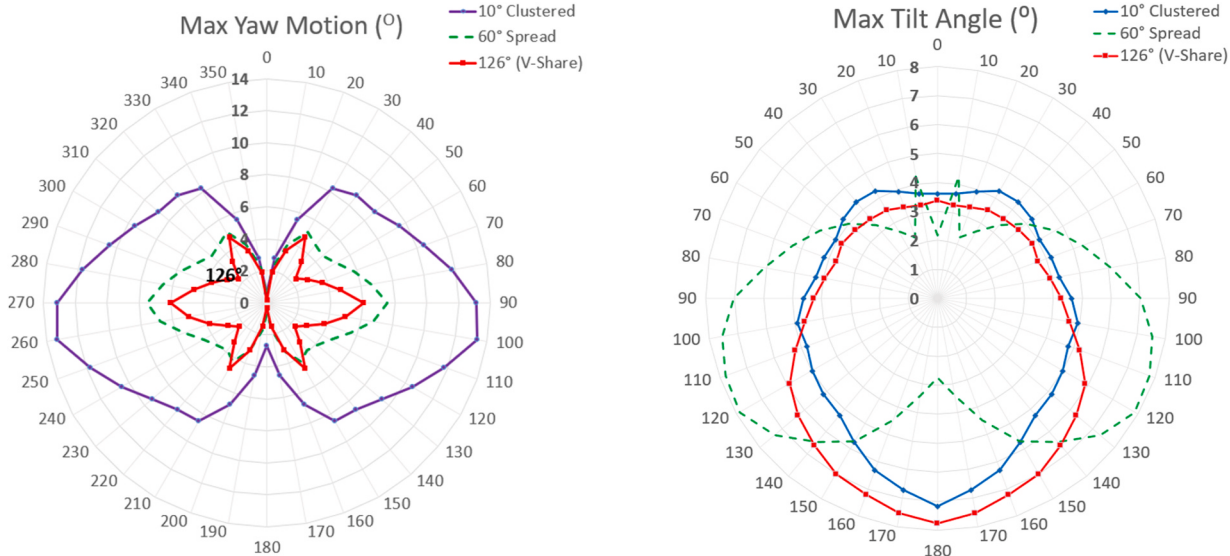


Fig. 11. Maximum platform yaw and tilt angles under three mooring patterns.

integrity (Kim et al., 2014). Fig. 11 presents yaw motion results, showing a substantial reduction in yaw for the 126° V-Share mooring configuration, while the 10° clustered case exhibits the highest yaw motion. The maximum yaw angles for 10° Clustered, 60° Spread, and 126° (V-Share) configurations are 13.3°, 7.25°, and 6.1°, respectively. The 126° V-Share mooring reduces yaw motion by 55 % compared to the 10° clustered case.

Fig. 11 also presents the tilt angle, defined as the geometric sum of pitch and roll. In general, differences in heel among the configurations are minimal, as heel is primarily governed by platform stability and the additional buoyancy volume generated when the floater inclines. These factors depend on hull geometry and inclination direction, with only a minor influence from the mooring system. However, the 126° V-Share configuration exhibits the minimum maximum tilt angle at 7.06°, representing a 2 % slight decrease compared to the 10° clustered configuration.

Equation (3) indicates that the V-Share mooring increases yaw stiffness. To assess the impact of yaw motion on the line tension, a series

of static simulations were conducted while varying yaw angles, with no wind, wave, or current loads applied. Fig. 12 presents the resulting line tension and floater yaw moments at the maximum yaw angles observed in Fig. 12. The results confirm that higher yaw stiffness contributes to the increased tension in the 126° V-Share configuration, as also reflected in Fig. 12.

Fig. 13 presents the MPM turbine tower bending moments, which are critical considerations in FOWT structural and tower design (Wu et al., 2023). The tower bending moments are mostly impacted by the tilt of the floater as well as dynamic acceleration. Both spread and V-Share mooring configurations reduce the maximum tower bending moment compared to clustered mooring, with the spread mooring giving the lowest tower bending moment. It is noted that tower modelling and configuration significantly impact tower bending moment; this remains an important topic for future research (Ma et al., 2025b).

The mooring pattern performances are summarized in Table 6. Overall, the V-Share mooring system reduces platform offset by 7 %, yaw motion by 55 %, and tower top bending moment by 17 %. The tilt

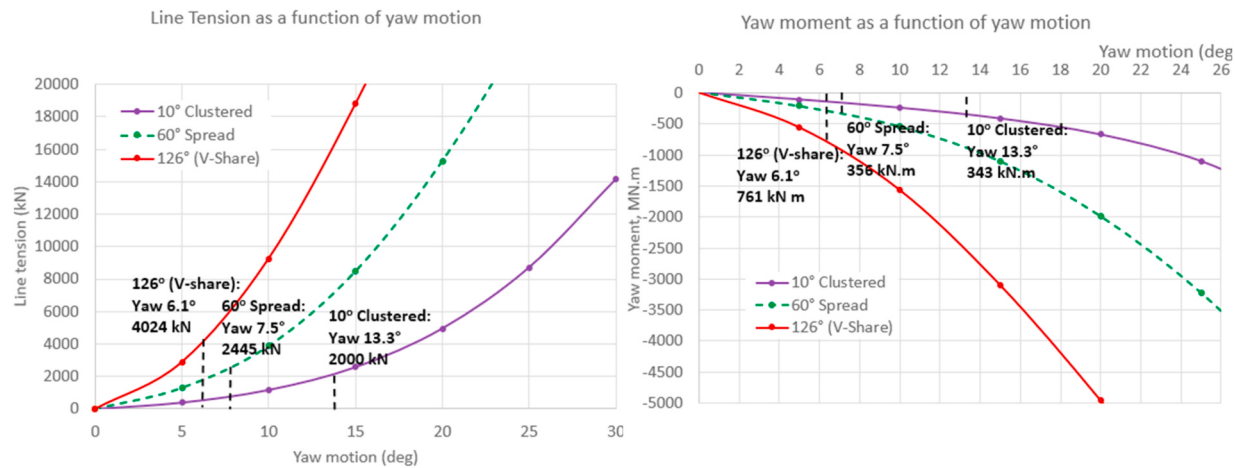


Fig. 12. Yaw-induced mooring tension and moment.

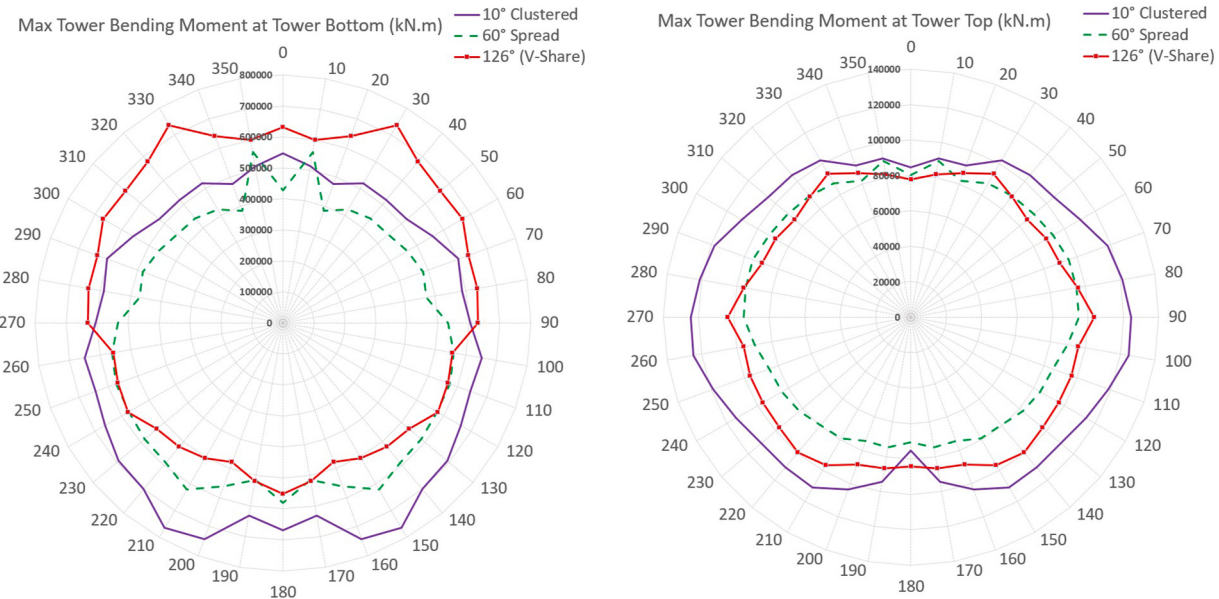


Fig. 13. Tower bending moments comparisons under three mooring patterns.

Table 6

Summary of mooring performance and floater motions comparisons under different mooring patterns.

Parameter	Unit	10° Clustered	60° Spread	126° V-Share
Maximum Tension (Intact)	kN	23,476	26,903	27,796
	Delta (%)	0 %	15 %	18 %
Maximum Offset	m	16.9	14.0	15.7
	Delta (%)	0 %	-17 %	-7 %
Maximum Yaw	deg	13.34	7.53	6.05
	Delta (%)	0 %	-44 %	-55 %
Maximum Tilt	deg	7.19	7.08	7.06
	Delta (%)	0 %	-1 %	-2 %
Maximum Tower Bending Moment at Tower Bottom	MNm	764,153	621,772	735,682
	Delta (%)	0 %	-19 %	-4 %
Maximum Tower Bending Moment at Tower Top	MNm	124,766	95,003	103,587
	Delta (%)	0 %	-24 %	-17 %

Table 7

Numerical analysis setup for the polynomial regression analysis of each mooring configuration.

Analysis ID	Pre-tension, % MBL	Pre-tension, kN	Chain diameter, mm
Bb	15	5827	220
Bm	10	3884	220
Bs	5	1942	220
Bxs	3.1	753	220
Mb	15	3642	160
Mm	10	2428	160
Ms	5	1214	160
Sxb	38.7	5827	120
Sb	15	2259	120
Sm	10	1506	120
Ss	5	753	120

angle is reduced slightly by 2 %. This indicates that the V-Share mooring will make the platform more stable. However, it also leads to an 18 % increase in maximum mooring tension.

To provide a preliminary insight into yaw effects on power production, a limited set of DLC 1.6 (ABS, 2020) simulations was performed

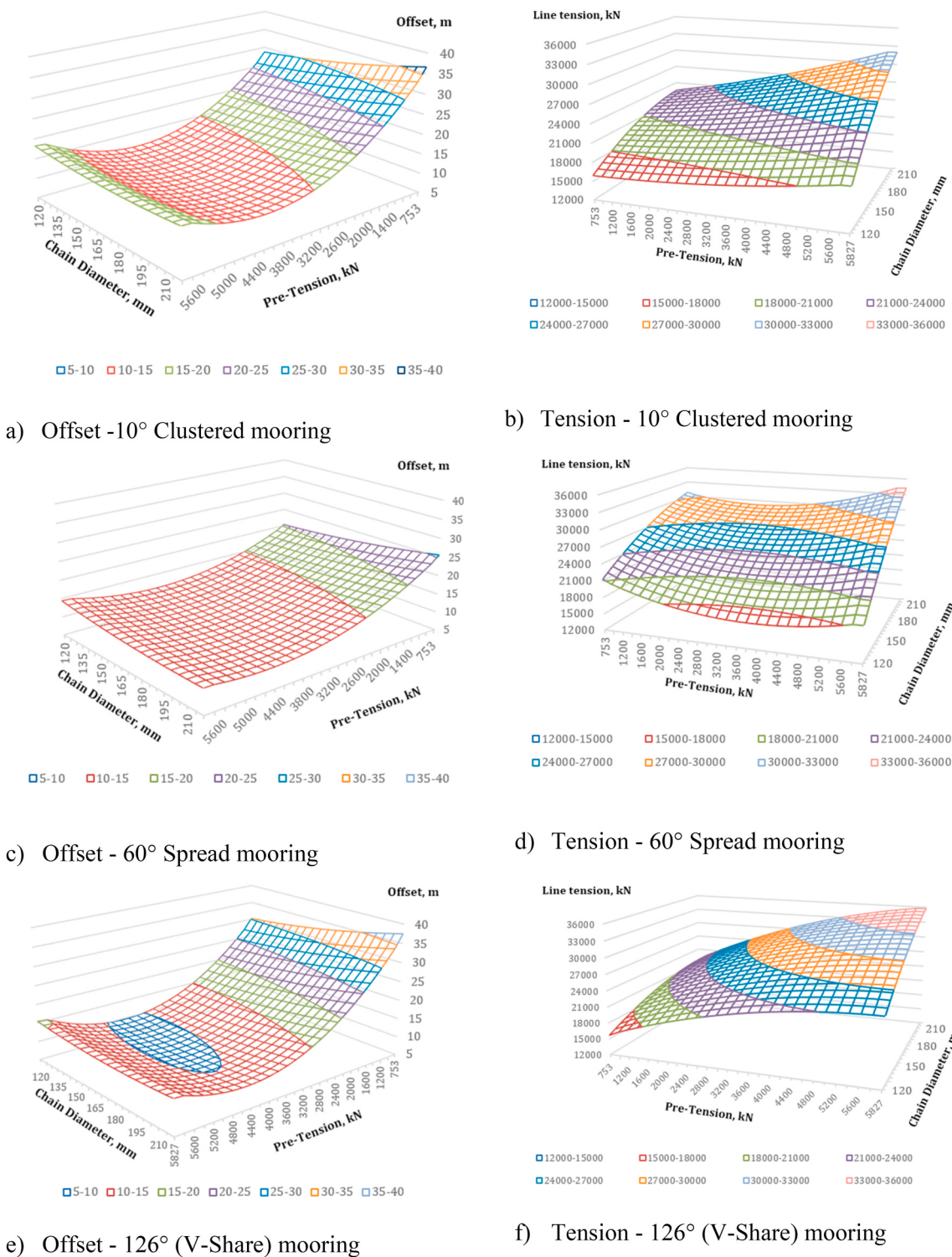


Fig. 14. Response surfaces for platform offset and mooring tension.

using a 10.59 m/s full-field wind input. The high-level estimation indicates that power output remains relatively stable up to yaw angles of approximately 8°, maintaining around 13,870 kW. Beyond this angle, the reduction in output is minor, with a minimum power of 13,680 kW, representing a 190-kW difference between the highest and lowest values. However, when extrapolated over 25 years of operation, assuming a 0.5 capacity factor, 0.9 efficiency, and an electricity price of USD 0.166/kWh (Taiwan), this small decrease could result in a loss of approximately USD 3.1 million in revenue, for a single FOWT.

Therefore, while more detailed analysis is needed for a fully accurate quantification, these results suggest that effectively limit yaw motion, such as the V-Share configuration, can contribute to long-term energy yield and project economics.

5.2. Mooring system optimization

In the simulations discussed above, a 160 mm chain diameter was used across all cases, resulting in varying offsets among different

Table 8

Response surface coefficients.

Case	Response surface coefficients					
	b0	b1	b2	b3	b4	b5
10° Clustered Offset	3.689E+01	-1.178E-02	-3.419E-02	1.798E-06	-1.772E-05	3.727E-04
10° Clustered Tension	-4.801E+03	-1.683E+00	2.359E+02	1.143E-04	1.168E-02	-5.252E-01
60° Spread Offset	2.559E+01	-5.367E-03	-3.906E-02	9.246E-07	-1.578E-05	3.035E-04
60° Spread Tension	1.444E+02	-5.313E+00	2.582E+02	4.928E-04	1.249E-02	-5.062E-01
126° V-Share Offset	4.097E+01	-1.322E-02	-5.027E-02	1.875E-06	-1.693E-05	3.987E-04
126° V-Share Tension	-6.248E+03	2.555E+00	2.191E+02	-3.194E-04	1.054E-02	-4.918E-01

Table 9

Optimized mooring design for each mooring pattern.

Parameter	Unit	10° Clustered	60° Spread	126° (V-Share)
Optimal Pretension	% MBL	6.4 %	4.6 %	5.9 %
Optimal Chain Weight	mt	8536	10657	10453

mooring patterns. To ensure a fair cost comparison, all configurations are optimized to achieve the same 20 m offset limit.

To equalize offsets across configurations, pre-tension and mooring sizes were optimized in each mooring configuration. To achieve this, the traditional approach is iterative design – changing both pre-tension and chain diameter in small increments until the optimal solution is found. Because (i) the tension is very sensitive to small changes in these parameters, (ii) their interaction effect is present, (iii) for each iterations, many seeds and directions all have to be re-run, only a small number of iterations can be done, thus the optimal design is not achieved and comparison between mooring systems is not fair. This paper proposed finding the optimal solution using polynomial regression with response surface analysis.

To conduct polynomial regression with response surface analysis, a total of 11 cases of analysis for each mooring configuration were conducted, as shown in Table 7. A brute-force evolutionary solver was applied to fit the data to Equation (9) (Shanock et al., 2010) and generate response surfaces for offset and tension, as shown in Fig. 14. The brute-force solver in Microsoft Excel works to minimize the objective line weight function by varying input parameters (pre-tension and diameter) while subject to constraints (available chain diameter, floater offset, chain MBL). This solver employs a genetic algorithm approach, which iteratively refines a population of solutions through processes of selection, crossover, and mutation to find an optimal solution for non-smooth problems. The fitted coefficients as output from the solver are provided in Table 8.

The tension values presented in the figures exclude pre-tension, as it is treated as an input variable; this component is reintroduced in the final step when assessing chain cost. The response surface is further analyzed to determine the minimum chain weight required for each configuration, varying pre-tension and diameter while ensuring that offset remains within the design limits and that factored tension (including the safety factor) stays within MBL limits. The results of optimization analysis are tabulated in Table 9.

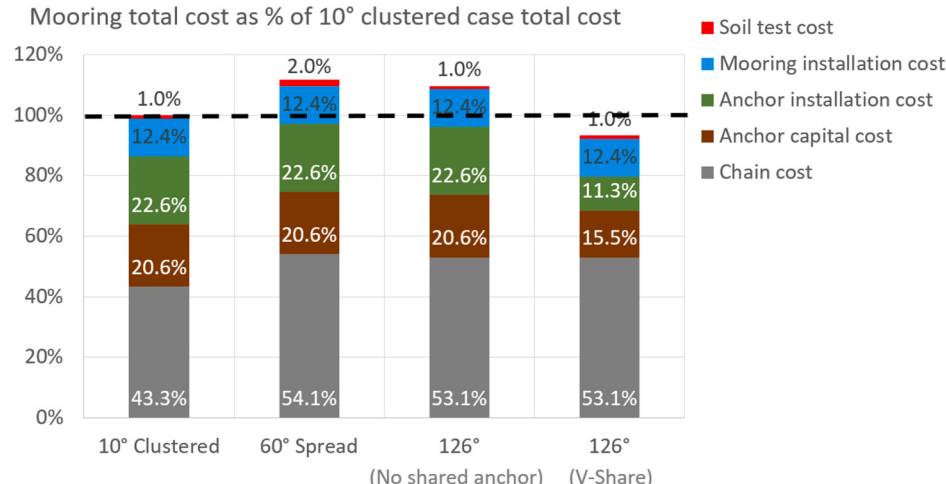
While offset response surfaces exhibit similar trends, tension response surfaces differ significantly. Mooring line stiffness consists of both elastic stiffness (dependent on chain length and diameter) and geometric stiffness (determined by pre-tension and spreading angle). Although spreading angle slightly affects elastic stiffness by increasing line length (up to 2.5 %), it has a much greater impact on geometric stiffness, leading to noticeable differences in tension response surface shapes.

The fact that the four corners of each response surface are all located at different heights shows that a significant interaction effect is present, so linear prediction approaches (when chain diameter and pre-tension are varied separately) are not suitable to predict the performance of a mooring system.

5.3. Cost analysis

The cost analysis is conducted for the mooring system, including procurement, installation, and soil test costs. It considers only mooring-related expenses and excludes floaters' costs. Consequently, the potential for the V-Share mooring system to optimize floater design is not accounted for in this analysis.

For the 126° configuration, a cost comparison is made between a clustered mooring without a shared anchor, where two separate but closely spaced anchors are used, and a V-Share mooring, where two mooring lines connect to the same anchor. In the V-Share configuration, the anchor size increases, but by less than double compared to

**Fig. 15.** Cost comparison of the three mooring patterns.

traditional mooring. As a preliminary estimate, this study assumes a 50 % increase in anchor size when two mooring lines share the same anchor (Wu et al., 2023).

Fig. 15 presents the cost comparison of different mooring configurations, using the total cost of the 10° configuration as the baseline (100 %). Results show that the 10° clustered configuration has the lowest chain material cost and thus the most cost-efficient among the three configurations if the shared anchor is not used. In contrast, the 60° spread mooring is the least economical. However, with anchor sharing, the V-Share mooring becomes more cost-effective than the 10° configuration, achieving about 10 % cost saving for a stand-alone floater.

It is expected that for a large-scale wind farm, anchor sharing is expected to further reduce overall project costs, making the V-Share mooring system even more cost advantageous.

6. Conclusions

This paper introduces and evaluates the V-Share mooring system for floating offshore wind turbines in harsh environments, with strong wind, wave, or current conditions. A comparative study was conducted between the proposed V-Share mooring and two conventional mooring configurations: (1) clustered mooring, where adjacent lines within each cluster are separated by 10°, and (2) spread mooring, where adjacent lines are separated by 60° evenly. The comparison is based on a 15 MW semi-submersible floating offshore wind turbine (FOWT) deployed in a typhoon-prone environment, using fully coupled mooring analyses with an all-chain mooring system. For each mooring configuration, this paper presents a novel optimization approach by applying polynomial regression with response surface analysis to identify optimal mooring design parameters, pretension, and chain size for each configuration.

The results demonstrate that the V-Share mooring system improves floater stability by reducing platform offsets by 7 % and yaw motions by over 50 %. However, due to its higher yaw stiffness, it leads to increased mooring tensions by 18 %, compared to the other two configurations in this study. A mooring system optimization was performed for each configuration using polynomial regression analysis, and the cost analysis demonstrated that the V-Share mooring system is the most cost-efficient solution, primarily due to the shared anchor design.

A shared anchor connecting two or three mooring lines among different floaters is a field-proven design, such as the Hywind Tampen project. However, connecting two mooring lines from a single floater to one anchor is novel. Therefore, the anchor design for V-Share mooring, suitable for the anticipated loads, and the availability of vessels and methods to deploy these anchors, remains a promising area for future research and development.

Although this study investigates the V-Share mooring system for a single floater, the concept shows strong potential for application in multi-turbine floating wind farms. Sharing anchors between adjacent floaters could significantly reduce the total number of anchors and the extent of geotechnical site investigations, thereby lowering project costs and environmental impact. In large-scale deployments, anchor systems may need to support up to six mooring lines in non-shared-line configurations, or up to twelve lines if shared mooring lines are used. These configurations introduce additional challenges for anchor design. Furthermore, if shared mooring lines are adopted, the resulting dynamic interactions between platforms and potential wake interference merit further investigation.

The V-Share mooring system allows for the mooring installation procedure to be optimized (Wu et al., 2023). The evolution of V-Share mooring technology can influence the cost of mooring system for floating wind. The V-Share mooring offers a reduced mooring footprint, minimizes seabed disruption, and provides a pathway to optimizing installation procedures and reducing hook-up duration. All of these can be important from a practical engineering perspective.

This study utilizes a large chain size for the semi-submersible, Tai-daFloat, which features an asymmetric off-column design. Given the

substantial chain size required in this study, further increasing the chain diameter may be necessary to achieve the desired safety factors and offset across all three configurations. The maximum mooring tension results indicate that an R4S-grade chain with a 220 mm diameter would be required to meet the targeted safety factors, a size that is beyond the current industry comfort zone. However, scaling up the chain size may not be the most cost-efficient solution. Previous studies on semi-taut mooring systems using fiber ropes have shown that the V-Share mooring system results in only 2–10 % higher tension compared to conventional designs (Wu et al., 2023), with significantly lower tension in deep water.

This study focuses on mooring tension and platform motions, with numerical simulations serving as the basis for performance comparisons. However, mooring fatigue remains a critical concern that should be addressed in future research. While numerical simulations provide valuable insights, model testing may be beneficial for verifying mooring performance and platform motions. Additionally, this study used an off-center column as the turbine location. A center-column arrangement may have a smaller yaw motion, thus diminishing the negative impact of yaw on mooring tension. There can be benefits of central column location for large-scale turbines, and therefore, its effect on mooring tension needs to be explored in the future.

CRediT authorship contribution statement

Glib Ivanov: Writing – original draft, Validation, Software, Investigation, Formal analysis, Data curation, Conceptualization. **Yongyan Wu:** Writing – review & editing, Writing – original draft, Supervision, Resources, Methodology, Investigation, Conceptualization. **Kai-Tung Ma:** Writing – review & editing, Supervision, Conceptualization.

Declaration of competing interest

The authors declare that they have no known competing financial interests or personal relationships that could have appeared to influence the work reported in this paper.

Acknowledgements

The authors from National Taiwan University gratefully acknowledge financial support from the Taiwan National Science & Technology Council (Grant No. 111-3116-F-002-007) and the Taiwan Ministry of Education's Yushan Fellow Program (Grant No. 112V1005-3). The second author thanks Aker Solutions management team for supporting the publication of this paper and knowledge-sharing with the community. The first author also extends sincere appreciation to Mr. DongHui Chen from Genesis Engineering, Houston, Texas, for his valuable insights and to Mr. Zhao-Yu Lai for providing the floater's motion RAO data.

References

- ABS, 2020. Guide for Building and Classing Floating Offshore Wind Turbines.
- Aryawan, Iwan, McEvoy, Paul, Kim, Seojin, Faria, Rui Pedro, 2023. Potential mooring system optimization using polymer spring component – floating offshore wind turbine application. In: Paper Presented at the Offshore Technology Conference, Houston, Texas, USA. <https://doi.org/10.4043/32410-MS>.
- Chang, H.-C., Ma, K.-T., Wang, C.-W., Liu, C., Hsiao, Y.-S., Wu, H.-P., Hsu, I.-J., Ivanov, G., Chiang, M.-H., 2022. Prospects of offshore wind power in Taiwan and the development of semi-submersible floating platforms. In: Taiwan Wind Energy Symposium, Tainan, Taiwan. https://www.researchgate.net/publication/364955126_taiwanlianfengdianzhiqujianqingyubanqianshifutazhifazhan.
- Díaz, H., Guedes Soares, C., 2020. Review of the current status, technology and future trends of offshore wind farms. Ocean Eng. 209, 107381. <https://doi.org/10.1016/j.oceaneng.2020.107381>.
- Fonseca, N., Førre, H.M., Sørum, S.H., Gaarder, R., Leira, B.J., Faria, R.P., Kent, M., 2024. Nylon Ropes for Mooring of Floating Offshore Wind Turbines: the NYMOOR Project. <https://doi.org/10.1115/OMAE2024-130846>. OMAE2024-130846.
- Hasumi, T., Yokoi, T., Haneda, K., Chujo, T., Fujiwara, T., 2023. Estimation for efficiency of offshore installation process of floating offshore wind turbines in Japan. In: 42nd

- International Conference on Ocean, Offshore and Arctic Engineering. ASME, Melbourne, Australia.
- Hong, S., McMorland, J., Zhang, H., Collu, M., Halse, K.H., 2024. Floating offshore wind farm installation, challenges and opportunities: a comprehensive survey. *Ocean Eng.* 304, 117793. <https://doi.org/10.1016/j.oceaneng.2024.117793>.
- Huang, J., et al., 2024. Analysis of mooring performance and layout parameters of multi-segment mooring system for a 15 MW floating wind turbine. *Front. Energy Res.* 12, <https://doi.org/10.3389/fenrg.2024.1502684>.
- IEA Wind TCP 37, 2020. System Engineering in Wind Energy – WP 2.1 Reference Wind Turbines.
- Ivanov, G., Poita, Y., 2025. Ensuring the security of onshore and offshore wind farms in the context of war or terrorism. *Sustain. Marine Struct.* 7 (2), 45–62. <https://doi.org/10.36956/sms.v7i2.1865>.
- Ivanov, G., Hsu, I.-J., Ma, K.-T., 2023. Design considerations on semi-submersible columns, bracings and pontoons for floating wind. *J. Mar. Sci. Eng.* 11, 1663. <https://doi.org/10.3390/jmse11091663>.
- Ivanov, G., Ma, K.-T., 2024a. Floater assembly and turbine integration strategy for floating offshore wind energy: considerations and recommendations. *Wind* 4 (4), 376–394. <https://www.mdpi.com/2674-032X/4/4/19>.
- Ivanov, G., Hsu, I.J., Ma, K.T., 2024b. Overview of FOWT demo projects cost and analyses of hull design features. In: Proceedings of the Third World Conference on Floating Solutions. Springer Nature Singapore, Singapore. https://doi.org/10.1007/978-981-97-0495-8_44.
- Jonkman, B.J., 2016. Turbsim User's Guide Version v2.00.00. NREL.
- Kim, M.G., Dalhoff, P.H., 2014. Yaw systems for wind turbines – overview of concepts, current challenges and design methods. *J. Phys. Conf.* 524 (1), 012086. <https://doi.org/10.1088/1742-6596/524/1/012086>.
- Lai, Z.-Y., Ivanov, G., Chen, J.-C., Chen, D., Ma, K.-T., 2024. Mooring anchor radius and spread-angle optimization for a 2 MW semi-submersible floating wind turbine in Taiwan strait. In: International Conference on Ocean, Offshore and Arctic Engineering (OMAE 2024). American Society of Mechanical Engineers, Singapore.
- Lee, C.-I., Chen, T.-L., Lin, T.-Y., 2024. Experiment on hydrodynamic characteristics of A semi-submersible floating platform. In: 1st Asia Pacific Conference on Offshore Wind Technology (APCOW 2024). Fukuoka, Japan.
- Lozon, E., Hall, M., 2023. Coupled loads analysis of a novel shared-mooring floating wind farm. *Appl. Energy* 332, 120513. <https://doi.org/10.1016/j.apenergy.2022.120513>.
- Lozon, E., Lekkala, M.R., Sirkis, L., Hall, M., 2025. Reference mooring and dynamic cable designs for representative U.S. floating wind farms. *Ocean Eng.* 322, 120473. <https://doi.org/10.1016/j.oceaneng.2025.120473>.
- Ma, K.T., Shu, H., Smedley, P., L'Hostis, D., Duggal, A., 2013. A historical review on integrity issues of permanent mooring systems. Offshore Technology Conference, Houston, TX. <https://doi.org/10.4043/24025-MS>.
- Ma, K.-T., Luo, Y., Kwan, T., Wu, Y., 2019. Mooring System Engineering for Offshore Structures. Elsevier. <https://www.sciencedirect.com/book/9780128185513/mooring-system-engineering-for-offshore-structures>.
- Ma, K.-T., Wu, Y., Stolen, S., Bello, L., van der Horst, M., Luo, Y., 2021. Mooring Designs for Floating Offshore Wind Turbines Leveraging Experience from the Oil & Gas Industry. OMAE. American Society of Mechanical Engineers. <https://doi.org/10.1115/OMAE2021-60739>.
- Ma, K.-T., Huang, W.-Y., Wu, K.-Y., Ivanov, G., 2025a. Wind farm design with 15 MW floating offshore wind turbines in typhoon regions. *J. Mar. Sci. Eng.* 13 (4), 687. <https://doi.org/10.3390/jmse13040687>.
- Ma, L., Yang, D., Guo, H., Shen, X., Zhou, L., 2025b. Development and verification of dynamic structural model of wind turbine tower based on the geometrically exact beam theory. *Front. Energy Res.* 13, 2025. <https://doi.org/10.3389/fenrg.2025.1569659>.
- Meng, Z., Liu, Y., Qin, J., Sun, S., 2021. Mooring angle study of a horizontal rotor wave energy converter. *Energies* 14 (2), 344. <https://www.mdpi.com/1996-1073/14/2/344>.
- Orcina, 2023. Orcaflex Manual Version 11.4.
- Rehman, S., A, L.M., Alam, Md M., Wang, L., Toor, Z., 2023. A review of energy extraction from wind and ocean: technologies, merits, efficiencies, and cost. *Ocean Eng.* 267, 113192. <https://doi.org/10.1016/j.oceaneng.2022.113192>. ISSN 0029-8018.
- Shanock, L.R., Baran, B.E., Gentry, W.A., Pattison, S.C., Heggestad, E.D., 2010. Polynomial regression with response surface analysis: a powerful approach for examining moderation and overcoming limitations of difference scores. *J. Bus. Psychol.* 25 (4), 543–554. <https://doi.org/10.1007/s10869-010-9183-4>.
- Tong, H.-Y., Lin, T.-Y., Chau, S.-W., 2023. Normal operating performance study of 15 MW floating wind turbine system using semisubmersible taida floating platform in Hsinchu offshore area. *J. Mar. Sci. Eng.* 11, 457. <https://doi.org/10.3390/jmse11020457>.
- Wu, Y., Leitch, P., Pedersen, S., Nærum, E., 2023. A new mooring system for floating offshore wind turbines: theory, design and industrialization. In: Offshore Technology Conference, Houston, USA. <https://onepetro.org/OTCONF/proceedings-abstract/23OTC/1-23OTC/D011S012R004/519322>.
- Xu, K., Larsen, K., Shao, Y., Zhang, M., Gao, Z., Moan, T., 2021. Design and comparative analysis of alternative mooring systems for floating wind turbines in shallow water with emphasis on ultimate limit state design. *Ocean Eng.* 219, 108377. <https://doi.org/10.1016/j.oceaneng.2020.108377>.
- Xu, H., Rui, S., Shen, K., Jiang, L., Zhang, H., Teng, L., 2024. Shared mooring systems for offshore floating wind farms: a review. *Energy Rev.* 3 (1), 100063. <https://doi.org/10.1016/j.enrev.2023.100063>.
- Yang, Y., Peng, T., Liao, S.J., 2023. Predicting 3-DoF motions of a moored barge by machine learning. *J. Ocean Eng. Sci.* 8 (4), 336–343. <https://doi.org/10.1016/j.joes.2022.08.001>.
- Yu, Y., Zhao, M., Li, Z., Zhang, B., Pang, H., Xu, L., 2024. Optimal design of asymmetrically arranged moorings in a floating production system based on improved particle swarm optimization and RBF surrogate model. *Mar. Struct.* 94, 103576. <https://www.sciencedirect.com/science/article/pii/S0951833924000042>.